XVIII International Conference on Water Resources
CMWR 2010
J. Carrera (Ed)

IMPACT OF CAPILLARY FORCES ON LARGE-SCALE MIGRATION OF CO_2

Jan M. Nordbotten[*,†], **Helge K. Dahle**[*]

[*]Department of Mathematics
University of Bergen, Bergen, Norway
e-mail: jan.nordbotten@math.uib.no
e-mail: helge.dahle@math.uib.no

[†]Department of Civil and Environmental Engineering
Princeton University, Princeton, NJ, USA

Key words: vertical equilibrium, capillary pressure, carbon storage

Summary. In this paper we derive closed-form constitutive functions for a vertically integrated model including gravitational and capillary forces. Such models are appropriate for CO_2 storage, and we use our derived functions to show the impact of capillary forces on tip migration speed. A particularly striking aspect is how capillary forces, while entering dispersive terms in the the fine-scale three-dimensional equations, appear in non-linear self-sharpening terms in the integrated equations. We highlight the physical interpretation of this change in character of the equations in the discussion.

1 INTRODUCTION

In the context of geological storage of CO_2, vertically integrated forms of governing equations in porous media have been gaining interest. Vertically integrated models coupled with a sharp interface assumption were initially applied to analyze the injection phase [7, 6]. This analysis was extended to more complex systems, with an emphasis on leakage and risk [9, 10]. Subsequently, sharp interface models were applied in the context of long term plume migration, particularly considering sloping formations [2, 3], and flow of background fluids [4]. Recent work has also looked at numerical solutions to the vertically integrated equations, with application to real field data [1].

While sharp interface models are attractive due to their simplicity, they neglect the impact of capillary forces on the fluid distribution. This omission is important if capillary forces lead to a transition zone that is appreciable on the scale of the aquifer, and if the fluid flow is slow enough to allow this transition zone to form. The former of these conditions is satisfied for many plausible injection sites of CO_2, while the latter condition will usually be satisfied for late-time buoyant migration.

Inclusion of capillary forces in vertically integrated models has a history in the petroleum literature (see e.g. [5, 11]). Recently the authors revisited these models, and considered their impact on plume evolution during injection, flow to a leaking well, and finally migration under a sloping aquifer [8]. This study showed that the capillary fringe may have a strong impact on CO_2 migration.

A drawback with including capillary forces in vertically integrated models is that the upscaled pseudo-functions become significantly more complex, and in particular, the pseudo-capillary-pressure-saturation relationship is defined through its inverse. Thus, the pseudo-functions are usually calculated numerically. The lack of analytical expressions for the pseudo-functions clouds our insight into the impact of fine scale processes on the integrated scale.

Here, we look at a vertically integrated formulation with capillary and buoyant forces. Using a particular choice of capillary-pressure-saturation and relative permeability curves on the fine scale, we are able to calculate analytically the integrated pseudo-functions. With these pseudo-functions, we analyze the impact of the capillary forces on the fine scale on the tip speed for upslope plume migration.

2 Model Equations

The vertically integrated equations for porous media have the same structure as the fine scale equations [5, 8]. Thus for two-phase immiscible, incompressible flow we can write mass conservation as

$$\Phi \frac{\partial S_\alpha}{\partial t} + \nabla \cdot U_\alpha = 0, \tag{1}$$

where the Darcy flux vector is given by

$$U_\alpha = -K\Lambda_\alpha(S_\alpha)(\nabla P_\alpha - \rho_\alpha G). \tag{2}$$

Here we note that capital letters denote the coarse scale variables, which are integrated porosity (Φ), average saturation (S_α) of phase α, integrated permeability K, coarse mobility Λ, bottom-aquifer pressure P_α and gravity G. The phases will be denoted $\alpha = w$ for wetting (brine) and $\alpha = n$ for non-wetting (CO_2).

Our emphasis in this paper is the pseudo-functions, and we will therefore simplify the system by assuming that the aquifer is flat with a tilt θ, and that the coordinate system is aligned with the tilt. Then we define the coarse pressure as the pressure at the bottom of the aquifer, and the mobility and gravity terms are defined as

$$\Lambda_\alpha \equiv K^{-1} \int_0^H k\lambda_\alpha(\hat{s}_\alpha)dz \quad \text{and} \quad G \equiv -g\sin\theta\nabla x \tag{3}$$

In this notation, the aquifer bottom is aligned with $z = 0$, while the top of the aquifer is $z = H$. Fine scale functions are denote by small letters, permeability (k) and mobility λ. We have denoted a saturation distribution by $\hat{s}_\alpha$. This is the critical object of modeling.

If the saturation is assumed to be strictly segregated by a sharp interface, so that $\hat{s}_\alpha$ is a (scaled) Heaviside function of z, then the integral simplifies such that the mobility is directly proportional to the region with fluid α, in other words $\Lambda_\alpha(S_\alpha) \sim S_\alpha$. Conversely, we will be interested in the case where the vertical saturation distribution is obtained from a balance of capillary and gravitational forces.

2.1 Capillary fringe pseudo-functions

Consider fluids in equilibrium, and denote the coarse fluid pressure as the pressure at the bottom of the aquifer $P_\alpha = p_\alpha(z = 0)$. Then, for constant density fluids, the vertical pressure distribution is

$$p_\alpha(z) = P_\alpha - \rho_\alpha g z. \tag{4}$$

If the fluids also honor the capillary-pressure-saturation curve, denoted $p^{cap}(s) = p_n - p_w$, we have that the saturation must satisfy

$$p^{cap}(\hat{s}(z)) = P^{cap} + \Delta\rho g z. \tag{5}$$

Here we have denoted the pressure difference as $\Delta\rho \equiv \rho_w - \rho_n$, which will be positive for our fluids. Physically measured capillary-pressure-saturation curves, while hysteretic, are always monotonic, so we will assume this function is (locally) invertible, and also write the inverse function as s^{cap}. By inverting Equation (5) we have the vertical saturation distribution

$$\hat{s}_\alpha(z) = s_\alpha^{cap}(P^{cap} + \Delta\rho g z). \tag{6}$$

From this, the coarse (average) saturation can be defined, so that

$$S_\alpha = \frac{1}{H}\int_0^H \hat{s}(z)dz. \tag{7}$$

By eliminating $\hat{s}$ from equations (6) and (7), the coarse capillary-pressure-saturation functions can be obtained; S^{cap}, which can be shown to be monotone, and therefore also P^{cap} exists. With these functions, and Equations (3) and (6), all coarse pseudo-functions can be defined.

3 Example calculation of analytical pseudo-functions

In general, the P^{cap} can not be obtained analytically from equations (6) and (7), and a numerical implementation is necessary. This is straight-forward, however intuition is lost. Fortunately, an important special case, which is physically reasonable, can be solved analytically. We present this calculation here.

We set the fine scale capillary pressure as

$$p^{cap}(s_n) = \alpha(1 - s_n)^{-1/2} + \beta. \tag{8}$$

We observe that $\gamma \equiv \alpha + \beta$ is the entry pressure. The fine scale mobility functions are given as

$$\lambda_w(s_n) = \lambda_c s_n^p. \tag{9}$$

and

$$\lambda_w(s_n) = \lambda_b(1 - s_n)^q. \tag{10}$$

Here λ_b, λ_c, p, and q are given parameters. These functional forms of capillary pressure and mobility are not uncommon in practice.

3.1 Coarse capillary pressure

Our first observation is that from Equation (5) and (8), we have that

$$\alpha(1 - s_n)^{-1/2} + \beta = P_c + \Delta\rho g z. \tag{11}$$

From this, we can define the interface ζ which corresponds to the saturation $s_n = 0$, or the bottom of two-phase region,

$$\gamma = P_c + \Delta\rho g \zeta, \;\; 0 \le \zeta \le H. \tag{12}$$

To proceed, define the following dimensionless parameters

$$B = \frac{\Delta\rho g H}{\alpha}. \tag{13}$$

and

$$P_*^{cap} = \frac{P^{cap} - \beta}{\Delta\rho g H}, \tag{14}$$

Note that P_*^{cap} is a dimensionless coarse scale capillary pressure, and B is a Bond number. We now turn to the approach outlined in Section 2.1. The inverse capillary function is given by

$$s_n^{cap} = 1 - \left(\frac{\alpha}{p^{cap} - \beta}\right)^2. \tag{15}$$

Combining Equations (6) and (15), and using the definition of dimensionless coarse capillary number, leads to

$$\hat{s}_n(P_*^{cap}) = \begin{cases} 0, & 0 \le \zeta, \\ 1 - B^{-2}\left(P_*^{cap} + \dfrac{z}{H}\right)^{-2}, & \zeta < z \le H. \end{cases} \tag{16}$$

When eliminating $\hat{s}_n$ from Equations (16) and (7), we need to take into account the two cases suggested by Equation (16):

(A): Assume that $\zeta = 0$. Then

$$S_n = \frac{1}{H}\int_0^H \left[1 - \frac{B^{-2}}{(P_*^{cap} + \frac{z}{H})^2}\right] dz = 1 + \frac{1}{B^2}\left[\frac{1}{P_*^{cap} + 1} - \frac{1}{P_*^{cap}}\right].$$

Hence

$$P_*^{cap} = \frac{1}{2}\left(-1 + \sqrt{1 + \frac{4B^{-2}}{1 - S_n}}\right). \tag{17}$$

Note that we chose the positive root because y has to be non-negative at least for some values of coarse scale saturation S_n. In particular, we may calculate the coarse-scale saturation when the capillary fringe first touches the lower aquifer plane. By Equation (12) and (14) we that $\zeta = 0$ implies $P_*^{cap} = B^{-1}$, from which the positive root in Equation (17) follows.

(B): Assume that $\zeta > 0$. Then

$$S_n = \frac{1}{H}\int_\zeta^H \left[1 - \frac{B^{-2}}{(P_*^{cap} + \frac{z}{H})^2}\right] dz = 1 - \frac{\zeta}{H} + \frac{1}{B^2}\left[\frac{1}{P_*^{cap} + 1} - \frac{1}{P_*^{cap} + \frac{\zeta}{H}}\right].$$

Solving the second-order polynomial leads to

$$P_*^{cap} = \frac{1}{2}\left(-[(2 - S_n) - 2B^{-1}] + \sqrt{[(2 - S_n) - 2B^{-1}]^2 - 4[(1 - S_n) - 2B^{-1} + B^{-2}]}\right). \tag{18}$$

Again, the positive root is the correct choice due to continuity.

We note in particular that the sharp interface model is obtained in the limit of negligible variation in capillary pressure, e.g. $\alpha \to 0$. Then $S_n = 1 - \zeta H^{-1}$ and $P_*^{cap} = S_n - 1$.

3.2 Coarse mobility

Given the coarse pseudo-capillary-pressure-saturation function, we can construct a fine-scale saturation distribution for any coarse scale saturation, using $P^{cap}(S_n)$ and Equation (6). This fine-scale saturation can be substituted into the definitions of the coarse mobility functions.

Assume that the permeability is constant in the vertical, so that permeability cancels from the definition of coarse mobility. Then for $\zeta = 0$ we obtain

$$\begin{aligned}
&\Lambda_n(P_*^{cap}) \equiv \frac{1}{H}\int_0^H \lambda_n(\hat{s}_n)dz = \frac{\lambda_c}{H}\int_0^H s_n^p dz = \lambda_c \int_0^H \left[1 - \frac{B^{-2}}{(P_*^{cap} + \frac{z}{H})^2}\right]^p dz = \\
&\lambda_c \int_0^1 \sum_{i=0}^{p} \binom{p}{i} (-1)^i B^{-2i} (P_*^{cap} + u)^{-2i} du = \\
&\lambda_c \sum_{i=0}^{p} \binom{p}{i} \frac{(-1)^i}{B^{2i}(1-2i)} \left[(BP_*^{cap} + B)^{1-2i} - (BP_*^{cap})^{1-2i}\right],
\end{aligned} \tag{19}$$

A similar calculation can be performed for $\zeta > 0$. Introducing the simplifying notation

$$Q(u, p) = \frac{1}{B^{2i}} \sum_{i=0}^{p} \binom{p}{i} \frac{(-1)^i}{1-2i} u^{1-2i}, \tag{20}$$

we can express the coarse non-wetting mobility as

$$\Lambda_n(S_n) = \begin{cases} \lambda_c \left[Q(P_*^{cap}(S_n) + 1), p) - Q(P_*^{cap}(S_n), p) \right], & \zeta = 0, \\ \lambda_c \left[Q(P_*^{cap}(S_n) + 1, p) - Q(B^{-1}, p) \right], & \zeta > 0. \end{cases} \tag{21}$$

For the wetting phase, the calculation is slightly more involved since we need to consider the polynomial expansion of $(1 - s_n)^q$. This is accomplished with using the binomial coefficients, such that we obtain

$$\Lambda_w(S_n) = \begin{cases} \lambda_c \sum_{i=0}^{q} \binom{q}{i} (-1)^i \left[Q(P_*^{cap}(S_n) + B, j) - Q(P_*^{cap}(S_n), j) \right], & \zeta = 0, \\ \lambda_c \sum_{i=0}^{q} \binom{q}{i} (-1)^i \left[Q(P_*^{cap}(S_n) + B, j) - Q(B^{-1}, j) \right], & \zeta > 0. \end{cases} \tag{22}$$

4 Plume migration

Of special interest may be the tip speed of the plume [2, 3, 4]. An estimate of the tip speed can be obtained by analyzing the fractional flow formulation for the coarse governing equations:

$$\frac{\partial \Phi S_n}{\partial t} + \nabla \cdot \{ F_n U - \Lambda_w F_n K \left[G + \nabla P_c \right] \} = 0. \tag{23}$$

Here U is the total flow, and F_n is the fractional flow function, defined by

$$F_\alpha = \frac{\Lambda_\alpha}{\Lambda_n + \Lambda_w}$$

It is well known from Buckley-Leverett theory that the solution to the fractional flow formulation can be approximated using the hyperbolic part of Equation (23). For the purposes of this discussion, the qualitative nature of the response is sufficiently captured by considering the case of constant flow with no slope (see e.g. [4]),

$$\frac{\partial S_n}{\partial t} + \nabla \cdot \{ F_n \} = 0. \tag{24}$$

Here we have, without loss of generality, scaled the system so that $\Phi/U = 1$. The well-known solution of Equation (24) is obtained by differentiating the convex hull of F_n. The tip speed is then obtained by considering the position x for which $S_n(x) = 0$.

In the sharp interface limit ($\alpha \to 0$), the fractional flow function is convex, and the tip speed is therefore given simply as

$$v_{tip}^{SI} = \left. \frac{dF_n}{dS_n} \right|_{S_n = 0} = \frac{\lambda_c}{\lambda_b}. \tag{25}$$

We see here that the plume tip speed can be estimated as simply proportional to the mobility ratio for the two fluids. We denote the sharp interface tip speed by superscript SI, and it represents the upper bound on the tip speed.

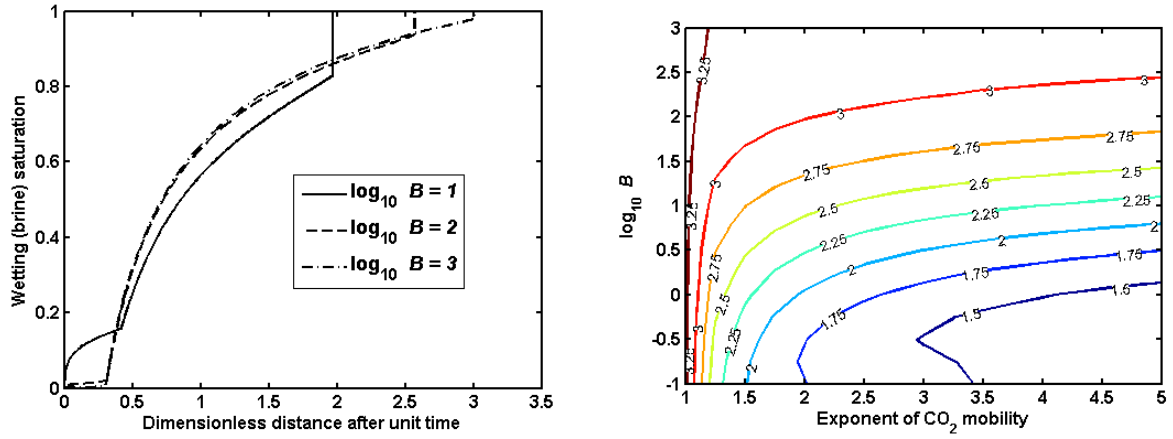

Figure 1: The left figure shows a contour plot of the tip speed as a function of the fine scale Bond number (B) and the non-linearity of the non-wetting mobility function, represented by its exponent. The exponent of the wetting phase mobility function was kept constant at $q = 3$. The right figure shows the corresponding (coarse scale) saturation profiles for different Bond numbers. For this figure, the mobility exponents were kept constant at $p = 2$ and $q = 3$. Note that the shock positions correspond to the contours in the left figure, as expected.

We will choose α as a measure of the span of the fine-scale capillary-pressure-saturation curve. When $\alpha > 0$ the fractional flow function loses convexity. The tangent line (for an initial condition with $S_n = 0$ and a boundary value above the shock saturation) is given by

$$\left.\frac{dF_n}{dS_n}\right|_{S_n=S_n^*} = \frac{F_n(S_n^*)}{S_n^*} \tag{26}$$

Here the shock saturation (which is the end-point of the tangent line) is denoted S_n^*.

Due to the structure of the coarse scale mobility functions, the Equation (26) cannot be calculated analytically. However, a numerical solution is straight forward.

In Figure 1 we have plotted the impact of fine-scale capillary pressure and the non-linearity of the CO_2 mobility on the tip speed of the plume, scaled by the total fluid velocity. In this figure, a mobility ratio of 3.3 was used, which fixes an upper bound on the tip velocity, according to Equation (25).

First, we note that the effect of capillarity is counter to common intuition: While capillary forces are dispersive on the fine scale, they lead to self-sharpening behavior, and slower tip speeds on the coarse scale. This is understood intuitively from the fact that the capillary pressure smears the saturation distribution, and that the intermediate saturations have lower mobility due to the non-linearity of the fine scale mobilities. This is emphasized by considering the abscissa of the figure, where we see that the tip speed is a strong function of the exponent (non-linearity) of the fine scale non-wetting mobility function, in particular for low Bond numbers, which correspond to a large impact of capillary forces.

The right part of Figure 1 shows three invasion patters associated with different Bond numbers. The highest Bond number, which is closest to the sharp interface model, has predominantly been used in literature. This figure emphasizes that not only the tip speed, but also the subsequent displacement pattern, is affected by the capillary forces.

REFERENCES

[1] Gasda, S. E., J. M. Nordbotten and M. A. Celia. Vertical Equilibrium with Sub-scale Analytical Methods for Geological CO_2 Sequestration, Special issue of *Computational Geosciences*, 13(4), 469-481, 2009.

[2] M. A. Hesse, H. A. Tchelepi, B. J. Cantwell and F. M. Orr. Gravity currents in horizontal porous layers: transition from early to late self-similarity. *Journal of Fluid Mechanics*, 577:363–383, 2007.

[3] M. A. Hesse, F. M. Orr, and H. A. Tchelepi. Gravity currents with residual trapping. *Journal of Fluid Mechanics*, 611:35–60, 2008.

[4] R. Juanes, C. W. MacMinn and M. L. Szulczewski. The footprint of the CO_2 plume during carbon dioxide storage in saline aquifers: storage efficiency for capillary trapping at the basin scale. *Transport in Porous Media*, 2009.

[5] L. W. Lake. Enhanced oil recovery. *Prentice-Hall*, 1989.

[6] J. M. Nordbotten and M. A. Celia. Analysis of plume extent using analytical solutions for CO_2 storage. In *Proceedings of the 16th conference on Computational Methods in Water Resources*, 2006.

[7] J. M. Nordbotten and M. A. Celia. Similarity solutions for fluid injection into confined aquifers. *Journal of Fluid Mechanics*, 561:307–327, 2006.

[8] Nordbotten, J. M. and H.K. Dahle. Impact of the capillary fringe in vertically integrated models for CO_2 storage submitted to *Water Resources Research*.

[9] J. M. Nordbotten, M. A. Celia, S. Bachu, and H. K. Dahle. Semi-analytical solution for CO_2 leakage through an abandoned well. *Environmental Science and Technology*, 39(2):602–611, 2005.

[10] J. M. Nordbotten, M. A. Celia, D. Kavetski and S. Bachu. A semi-analytical model estimating leakage associated with CO_2 storage in large-scale multi-layered geological systems with multiple leaky wells. *Environmental Science and Technology*, 43(3):743–749, 2009.

[11] Yortsos, Y. C., A theoretical analysis of vertical flow equilibrirum *Transport in Porous Media*, 18, 107-129, 1995.